3056–3063 Nucleic Acids Research, 1995, Vol. 23, No. 15 © 1995 Oxford University Press

Use of ultra stable UNCG tetraloop hairpins to fold RNA structures: thermodynamic and spectroscopic applications

Marco Molinaro and Ignacio Tinoco, Jr*

Department of Chemistry, University of California and Division of Structural Biology, Lawrence Berkeley Laboratory, Berkeley, CA 94720, USA

Received December 23, 1995; Revised and Accepted June 19, 1995

ABSTRACT

RNA molecules of >20 nucleotides have been the focus of numerous recent NMR structural studies. Several investigators have used the UNCG family of hairpins to ensure proper folding. We show that the UUCG hairpin has a minimum requirement of a two base-pair stem. Hairpins with a CG loop closing base pair and an initial 5'CG or 5'GC base pair have a melting temperature ~55°C in 10 mM sodium phosphate. The high stability of even such small hairpins suggests that the hairpin can serve as a nucleation site for folding. For high resolution NMR work, the UNCG loop family (UACG in particular) provides excellent spectroscopic markers in one-dimensional exchangeable spectra, in two-dimensional COSY spectra and in NOESY spectra that clearly define it as forming a hairpin. This allows straightforward initiation of chemical shift assignments.

INTRODUCTION

The number of high resolution NMR structures of RNA molecules is increasing steadily. Naturally, the molecules studied are becoming larger and therefore more spectroscopically complex. Unusual secondary structure interactions (1,2), tertiary RNA interactions (3–5) and RNA-ligand complexes (6–8) have all been investigated. The main needs for such complex, high resolution NMR structural studies of RNA include: (i) a minimum number of nucleotides; (ii) a single, stable conformation and (iii) clear spectral markers to begin analysis of two- and three-dimensional spectra. Recent publications on NMR structures have made use of the UNCG tetraloops to meet these needs (3,8). The UUCG tetraloop has also been used successfully to prevent aggregation of larger molecules (9). It has been known for several years now that the UNCG family of tetraloops is ultra stable (10). High resolution NMR studies of a UUCG hairpin done in our laboratory (11–13) have revealed the interactions that bring about this extra stability. But up to now, investigators using the UNCG hairpins have used it with four or more base pairs in the stem, possibly adding unnecessary nucleotides to their structure. We report that the UNCG family of hairpins has such high stability that a mere two base-pair stem is sufficient to ensure a high melting temperature (T_m; up to 55°C in 10 mM sodium phosphate, depending on sequence used). Also, the UNCG family of hairpins provides very clear spectral markers distinguishing it from the GNRA ultra stable tetraloop family. More specifically, the UACG tetraloop provides the best spectroscopic markers for structural NMR studies.

MATERIALS AND METHODS

Chemical synthesis of RNA

Oligoribonucleotides in Figure 1, except for the UUCG 12mer, were synthesized on an Applied Biosystems 381 oligonucleotide synthesizer with 2'-tertbutyldimethylsylil protected phosphoramidites provided by Milligen/Biosearch. Solid phase synthesis was done, as suggested by the manufacturer, with a 20-fold excess of phosphoramidite per coupling step as well as an increase in coupling time from 5 to 15 min. The final trityl group was removed for ease of purification. Base protecting groups were removed by incubation in NH_4OH/EtOH (3/1) at 55°C for 16 h. Deprotection of the 2'OH was carried out with fresh 1 M tert-butyl ammonium fluoride in tetrahydrofuran at a 40:1 molar ratio for 16 h at room temperature. The reaction was stopped with the addition of an equal volume of 0.1 M ammonium acetate and the volume reduced to half in a Speed-Vac. The deprotected RNA was then desalted using a G-10 column with 50 mM ammonium acetate (pH 6.8) as the eluent. The sample was then repeatedly lyophilized against water and finally dissolved in 0.5 ml of water for injection into an HPLC.

Enzymatic RNA synthesis

RNA oligonucleotides were transcribed from DNA templates using T7 RNA polymerase and were purified using denaturing gel electrophoresis (14). The yield of RNA for the UUCG 12mer was 35–70 μg/ml of reaction. The UACG 25mer, presented for comparison, yielded from 100 to 130 μg/ml of reaction. The oligonucleotide sequences were verified using base-specific RNases A, T1 and U2 (15).

HPLC purification

RNA from chemical synthesis was purified on a 15 × 0.5 cm DIONEX NUCLEOPAC anion exchange column using a 0–70%

* To whom correspondence should be addressed

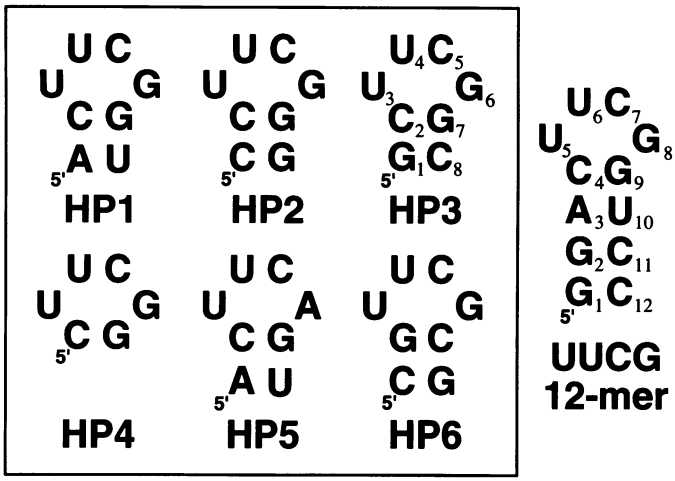

Figure 1. RNA sequences of chemically synthesized mini hairpins (outlined) and UUCG 12mer. Representative numbering is shown for HP3 and UUCG 12mer.

1.5 M ammonium acetate (pH 6.8) linear gradient. Up to 0.25 μmol of RNA were loaded per run without appreciable loss in resolution. Repeated lyophilization against water rid the sample of the ammonium acetate due to its volatility as ammonia and acetic acid. Final yields after purification of chemically synthesized RNA gave from 0.2 to 0.45 μmol of the desired 8mer from a 1 μmol theoretical maximum, this represented an overall coupling efficiency near 89% for the best case (coupling efficiency was more likely 92–93%, the figure given takes into account losses incurred during purification).

UV melting curves

The RNA samples used to measure UV melting curves were treated in two separate ways. Initial samples were not dialyzed due to fear of sample loss through the 1000 M.W. dialysis membranes, but instead repeatedly lyophilized then dissolved in 10 mM sodium phosphate buffer, pH 6.7–7.2 with 10 μM EDTA. To test if the lack of dialysis introduced error, HP1, HP3 and HP6 samples were dialyzed for 16 h (with <5% loss through the membrane) against 10 mM sodium phosphate, 10 μM EDTA, pH 6.8. There was no variation in melting temperature >0.5°C between dialyzed and non-dialyzed samples, well within experimental error. RNA concentrations varied from 10 μM to 1.11 mM. Samples were degassed under vacuum for 1 min and heated to 90°C for 2 min prior to collecting melt data. Four samples were run simultaneously on a Gilford 250 Spectrophotometer connected to a Fountain 286 PC for data acquisition. Heating was controlled by a Gilford 2527 Thermal programmer also connected to the PC. Samples were heated at either 0.5 or 1.0°C per min giving ~150–300 points per sample. The data were transferred to a Macintosh computer equipped with a Kaleidagraph for visualization and thermodynamic parameter quantitation.

Thermodynamic parameters were obtained by a six parameter non-linear least squares analysis based on the assumption of a unimolecular, two state transition from the hairpin to the single strand. The form of the equation used in the program was:

$$Absorbance = [e^{(-\Delta H^\circ/(RT))}e^{(\Delta S^\circ/R)}(m_1T+m_3)+(m_4+m_2T)]/(1+e^{(-\Delta H^\circ/(RT))}e^{(\Delta S^\circ/R)})$$

with T = temperature in K, m_1 = lower baseline slope, m_2 = upper baseline slope, m_3 = lower baseline intercept at 0 K, m_4 = upper baseline intercept at 0 K, ΔH° in cal/mol and ΔS° in cal/(K mol), R is the universal gas constant in cal/(K mol). Very rough initial values were input as a starting point for the fit.

NMR

Mini hairpins

Samples used for NMR were HPLC purified and dialyzed against 10 mM sodium phosphate, 10 μM EDTA, pH 6.8 for 16 h (longer times were avoided due to the small M.W. of the hairpin, ~2400, versus the 1000 M.W. cutoff of the dialysis membrane). Sample concentration for HP3 (Fig. 1) was 0.9 mM, for HP6 0.5 mM and for HP2 0.2 mM. Spectral referencing was to sodium 3-(trimethylsilyl)-1-propanesulfate (TSP) at 0.0 p.p.m. One- and two-dimensional spectra were taken on a Brucker AMX-600 spectrophotometer equipped with a Brucker UXNMR workstation. One-dimensional spectra were processed on the workstation; a μVAX running FT-NMR (Hare Research Inc.) was used to analyze two-dimensional spectra. Two-dimensional spectra were zero-filled to 1K real points prior to Fourier transformation, a 60–90° shifted sine bell was used in both dimensions for apodization. Non-exchangeable, one-dimensional spectra were taken with a sweep width of 5000 Hz from 5 to 70°C for determination of chemical shift melting curves as well as for selection of optimal temperature for two-dimensional experiments. One-dimensional exchangeable proton spectra were taken at 15°C with a sweep width of 11 500 Hz using 1331 water suppression. The sample was lyophilized and redissolved in a 90% H_2O/10% D_2O mixture to maintain the deuterium lock signal.

Phosphorus decoupled, double-quantum-filtered COSY spectra were collected at 5 and 35°C for HP3 and at 10°C for HP6, all with 2K points and a sweep width of 5000 Hz. Phosphorus decoupling was achieved with a spin-echo 180° ^{31}P pulse during t1 and with GARP decoupling (16). Relaxation delay was 2 s, 80–128 scans (depending on time available) were collected for each of 500–600 t1 values. The HDO peak was eliminated by presaturation during the relaxation delay.

NOESY spectra were collected at 5°C for HP3 with a sweep width of 5000 Hz. Approximately 350 FIDs of 2K points were acquired. The relaxation delay was 2 s, and 80 scans were averaged for each t1 value. The HDO peak was eliminated by presaturation during the relaxation delay and the 300 ms mixing time.

UUCG 12mer hairpin

The sample used for NMR was purified by gel electrophoresis and dialyzed against 10 mM sodium phosphate, 10 μM EDTA, pH 6.5 for >24 h. Detailed methods for this hairpin have been published (11).

UACG hairpin

The sample used for NMR was purified by gel electrophoresis and dialyzed against 10 mM sodium phosphate, 50 mM sodium chloride, 100 μM EDTA, pH 6.4 for 48 h. Spectra were acquired

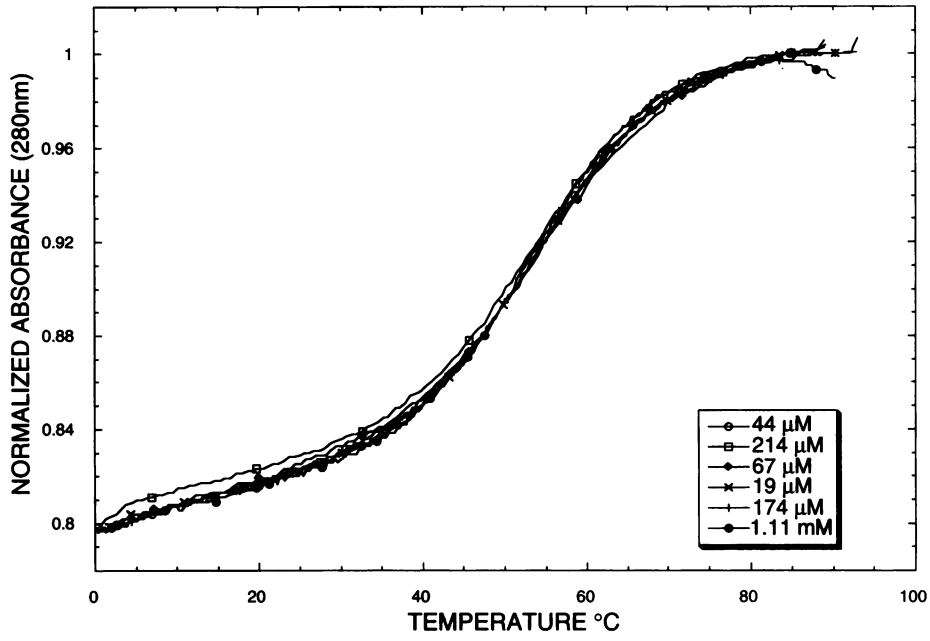

Figure 2. Normalized UV melting curves of HP3 from 19 μM to 1.11 mM in 10 mM sodium phosphate, 10 μM EDTA, pH 6.8. A marker is shown every 20th data point for clarity.

on a GE OMEGA-500 and the data processed with FELIX 2.1 running on an SGI workstation. One-dimensional exchangeable proton spectra were taken at 15°C with a sweep width of 10 000 Hz using 11 water suppression. A double-quantum-filtered COSY spectrum was taken at 15°C with a 5000 Hz sweep width and elimination of HDO peak with presaturation during the 2 s relaxation delay. 594 t1 increments of 2K real points were collected. The data were apodized in both dimensions with a skewed sinebell with a 50° shift and skew factor of 0.7. Spectral referencing was to TSP at 0.0 p.p.m.

RESULTS

Thermodynamics—UV melting curves

HP1, HP2, HP3. HP1, HP2 and HP3 all have a CG loop closing base pair and vary only in the initial base pair. These three hairpins were proven unimolecular from the independence of T_m on concentration (see Fig. 2 for overlap of HP3 melting curves), with T_ms of 37°C (HP1), 54°C (HP2) and 55°C (HP3) (Fig. 3). The T_m of HP2 and HP3 are within 16°C of their four base pair counterpart, the UUCG 12mer, 5′-GGACUUCGGUCC at 71.5°C.

HP4. This hairpin, with only one base pair in the stem, has no visible melting transition; it does not appear to form any secondary structure. A very low melting temperature, <5°C, cannot be ruled out (Fig. 3).

HP5. This hairpin was the only one tested that did not have the ultra stable UNCG tetraloop, but instead had a UUCA tetraloop. The melting curves show no apparent transition and therefore no secondary structure is likely to form. As expected, without the high stability of the UNCG loop, a two base pair stem does not lead to stable hairpin formation (Fig. 3).

HP6. This hairpin represents HP3 with each base pair in the stem reversed. Experimental data were difficult to fit due to lack of a lower baseline, but analysis of the derivative of the melting curve [the greatest slope on the curve is indicative of the melting temperature (17)] gave an approximate T_m of 24°C (Fig. 3).

Thermodynamics—nearest neighbor calculations

Nearest neighbor calculations with a loop bonus for the UNCG loop, and 5′ and 3′ stacking of the loop on the stem, predict T_m within 5°C of experimentally obtained values for all the hairpins that actually showed a transition (Table 1). ΔH° and ΔS° are not predicted as well and are underestimated from 10 to 30% (Table 1).

NMR

One dimensional non-exchangeable melting curves of HP3. The hairpin was followed from 5 to 70°C at 5°C intervals to determine if the loop was undergoing structural changes before the stem. The changes in chemical shifts showed transitions strongly correlated to the transition seen in the UV absorbance melting curves. The G1H8 and G7H8 protons in the stem showed a concurrent transition to the U4H1′ and C5H5 in the UUCG loop (Fig. 4). These results indicate that the stem and loop undergo the melting transition simultaneously: the transition is two state. Also, the transitions seen correlate strongly with what is observed using UV melting curves (Fig. 4).

Two dimensional non-exchangeable NMR of HP3. The methods used to assign the resonances in NMR spectra of RNA have been reviewed (18). The assignments from the 12mer UUCG hairpin (11) were used extensively to correlate to the HP3 chemical shifts (Table 2). The majority of sugar proton resonances were determined from a COSY spectrum at 5°C. The two C2′-endo sugars were assigned from observation of the large (>7 Hz)

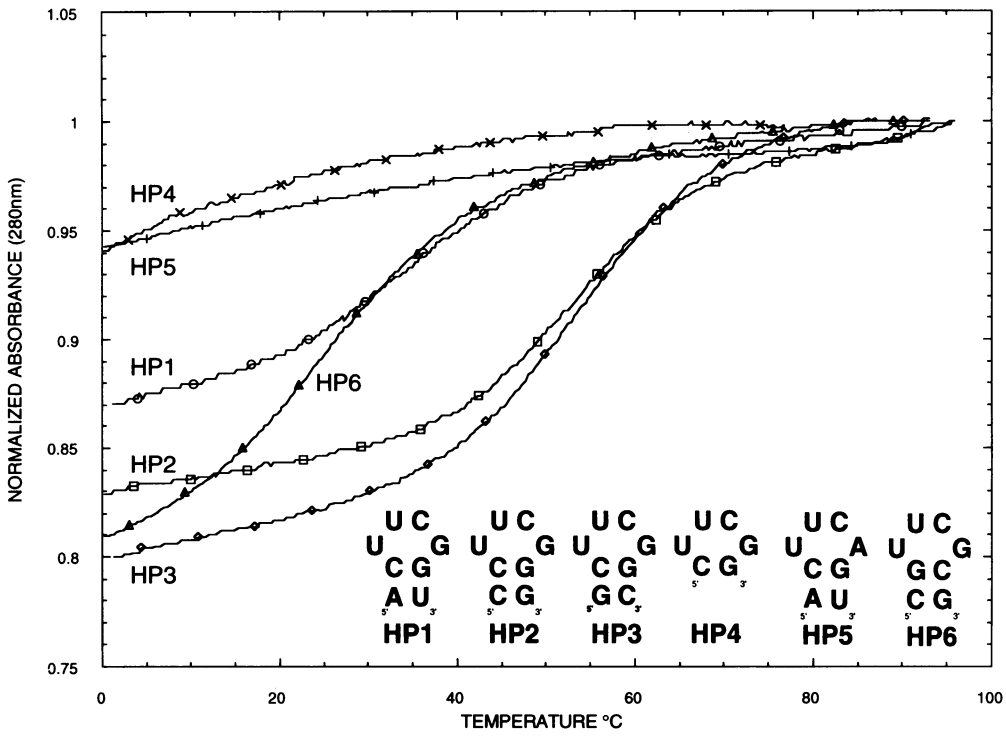

Figure 3. Normalized UV absorbance melting curves for HP1, HP2, HP3, HP4, HP5 and HP6. All samples are in the 20–40 μM concentration range. A marker is shown every 20th data point for clarity. All samples are in 10 mM sodium phosphate, pH 6.7–7.2, 10 μM EDTA.

Table 1. Experimental versus calculated thermodynamic parameters for HP1, HP2, HP3, HP4, HP5 and HP6. Experimental ΔH° and ΔS° values for HP1 and HP2 are ± 10%, for HP3 ± 5%. Calculated values are based on nearest neighbor numbers (24–26)

		HP1	**HP2**	**HP3**	**HP4**	**HP5**	**HP6**
	ΔG° calculated at :	**UC**	**UC**	**UC**	**UC**	**UC**	**UC**
	37.0 °C	**U G**	**U G**	**U G**	**U G**	**U A**	**U G**
		C-G	**C-G**	**C-G**	**C-G**	**C-G**	**G-C**
		A-U	**C-G**	**G-C**	**5' 3'**	**A-U**	**C-G**
		5' 3'	**5' 3'**	**5' 3'**		**5' 3'**	**5' 3'**
Experimental	ΔH°(kcal/mol)	-28.9	-34.5	-29.2			
	ΔS°(e.u.)	-93.1	-105.4	-88.9			derivative
	ΔG°(kcal/mol)	0.0	-1.8	-1.6			method
	Melting Temperature °C	36.8	54.1	54.9	<10	<10	≈24
Calculated	ΔH°(kcal/mol)	-21.9	-23.9	-25.9	-11.7	-17.9	-15.8
(using method	ΔS°(e.u.)	-70.7	-74.3	-79.5	-44.6	-64.3	-53.3
below)	ΔG°(kcal/mol)	0.0	-0.9	-1.2	2.1	2.1	0.7
	Melting Temperature °C	36.7	48.6	52.7	-10.7	5.1	23.4

EXAMPLE THERMODYNAMIC CALCULATIONS ON HP3 GC UUCG GC

U 5' GC U 3' CG C G	→ GC CG ←	→ CU G ←	→ C GG ←	4 member loop	UNCG tetraloop bonus	TOTAL
ΔH° kcal/mol	-14.2	-7.5	-0.2	0.0	-4.0	-25.9
ΔS° e.u.	-34.9	-20.4	0.0	-17.7	-6.5	-79.5
ΔG°kcal/mol	-3.4	-1.2	-0.2	5.5	-2.0	-1.2
				Melting Temperature °C		52.7

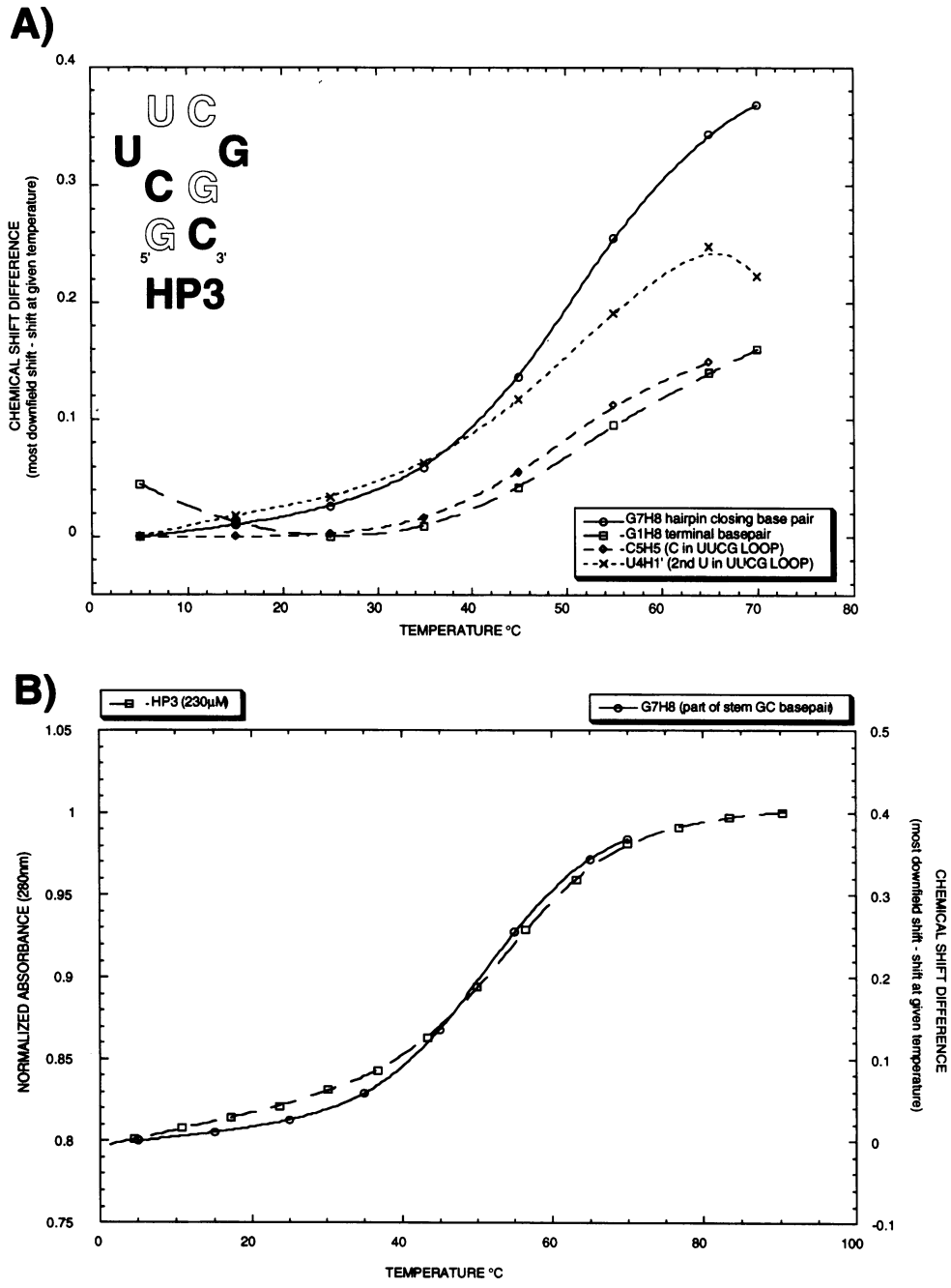

Figure 4. Chemical shift dependence on temperature versus UV melting curves for HP3. Chemical shift difference is calculated by subtracting the shift at a given temperature from the most downfield shift observed. (**A**) Chemical shift dependence of four resonances representing the stem and loop regions. Lines through points represent a smooth fit. (**B**) Comparison of UV and NMR melting curves. Solid line represents NMR data, jagged line represents UV melting data with every 20th data point shown with a marker.

coupling between H1′-H2′ as well as characteristic splitting patterns of the H2′-H3′ crosspeak. The absence of H1′-H2′ peaks indicated C3′-endo conformations for the rest of the sugars (C3′-endo H1′-H2′ coupling is ~1–2 Hz, not visible with the observed line width). C3′-endo characteristic H2′-H3′ peaks as well as H3′-H4′ peaks allowed unambiguous determination of H2′-H4′ spin systems.

The strongest peaks in the H1′-H2′ region of the NOESY data were assumed to be the H1′-H2′ cross-peaks. Combining the NOESY with the COSY data allowed H1′ through H4′ spin system determination for each C3′-endo sugar. The correlation of aromatics to H1′ shifts were done assuming A-form connectivities for G1-U3 and G6-C8 (see Fig. 1 for numbering of hairpins) in the aromatic to H1′ region and matching shifts with the UUCG

Table 2. HP3 chemical shifts. Shifts in bold correspond to strongly shifted resonances equivalent to those found in the UUCG 12mer. All non-exchangeable shifts are at 5°C referenced to 0 p.p.m. for TSP. Exchangeable shifts are at 15°C, similarly referenced

HP3 5°C	H8/H6	H5	H1'	H2'	H3'	H4'	H5'/H5"	IMINO at 15°c
1 G	8.09		5.82	4.11	4.16	4.20		13.40
2 C	7.75	5.32	5.72	4.68	4.44	4.55		
3 U	7.91	5.90	5.76	**3.89**	4.65	4.46		11.88
4 U	8.10	5.92	6.18	4.75	4.08			11.18
5 C	7.77	6.22	6.04	4.18	4.53		**3.67/2.76**	
6 G	7.91		6.01	4.88	**5.73**	4.47		9.96
7 G	8.38		< 5	4.50	4.29	4.43		13.53
8 C	7.62	5.36	5.73	4.47	4.23			

12mer for U3-G6. The C5 H5′/H5″ were also determined from similar NOE patterns to the UUCG 12mer. The G1 H8 shift correlated well with the location of 5′ terminal G's seen in other NMR studies (18). G6 had a very strong NOE to its own H1′ indicative of a syn nucleotide.

HP3 versus UUCG 12mer. Chemical shifts from the UUCG 12mer were used in determining HP3 assignments. In comparing chemical shifts, the greatest changes seen are in the 5′ end and carry through C2 and somewhat through U3 (refer to Fig. 1). This is reasonable considering HP3 has a G in the 1 position while the 12mer has an A in the equivalent position. The rest of the non-exchangeable chemical shifts differ by 0.08–0.13 p.p.m. The HP3 spectra were taken at a 20°C lower temperature than the UUCG 12mer reflecting the lower T_m of HP3, thus the chemical shift differences are reasonable. The exchangeable imino protons show a similar small shift, but in the opposite direction.

Overall there is a strong amount of evidence that HP3 forms a similar loop conformation to that found in the hairpin with the longer stem: (i) the two unpaired loop nucleotides, U4 and C5, both have C2′-endo sugar pucker (refer to Fig. 5A and B); (ii) all but the U3 aromatic shifts are within 0.1 p.p.m. of the 12mer; (iii) G6 is syn as evidenced by a very strong NOE to its H1′; (iv) U3H2′, C5H5′/H5″ and G7H1′ are all greatly shifted upfield as in the 12mer; (v) G6H3′ is shifted ~1 p.p.m. downfield from other H3′ protons (refer to Fig. 5A and B); (vi) relative NOE crosspeak intensities for equivalent resonances in the H1′ to aromatic and H2′ to aromatic regions of HP3 and the UUCG 12mer are identical (e.g. equivalent crosspeaks possess the same strong, medium or weak intensity). All of this evidence proved crucial in determining the 12mer loop conformation and therefore is very indicative of its special structure which is also present in HP3.

One and two dimensional non-exchangeable NMR of HP6. One-dimensional NMR spectra of HP6 at 5, 10 and 15°C are well dispersed with line widths comparable to HP3, except at 15°C, where broadening starts to occur as might be expected so close to the 23°C T_m. The characteristic upfield shifted C5H5′/H5″ of the 12mer and HP3 are present but broader. The downfield shifted G6 H3′ is also present. In the COSY spectrum, the central U and C in the loop are largely C2′-endo due to strong H1′-H2′ crosspeaks (J-coupling > 7 Hz). Based on this evidence, the overall loop

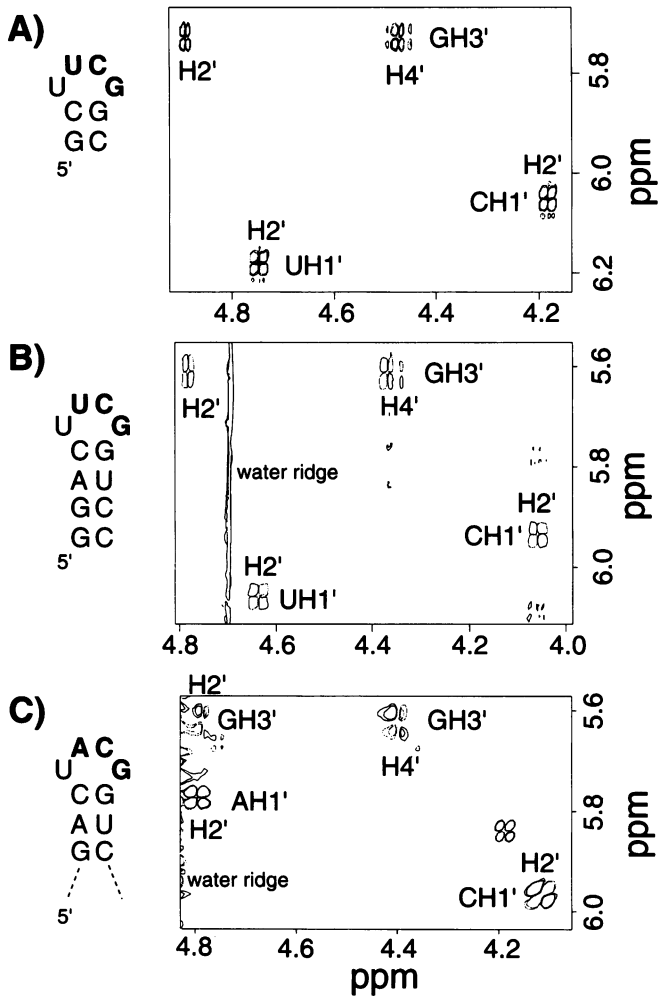

Figure 5. H1′-H2′ region of DQF-COSY spectra for HP3, UUCG 12mer and UACG 25mer. (**A**) HP3 crosspeaks at 5°C for C2′-endo central loop nucleotides and downfield shifted GH3′, bolded nucleotides refer to nucleotides marked in spectrum. Sample is in 10 mM sodium phosphate, 10 μM EDTA, pH 6.8. (**B**) As A except at 30°C for the UUCG 12mer and pH 6.5. (**C**) As A except at 15°C for the UACG 25mer and added 50 mM sodium chloride, pH 6.4. The water ridge at 4.85 p.p.m. interferes slightly with the GH3′-GH2′ crosspeak.

structure appears similar to that found in the UUCG loop of HP3 and the 12mer.

One dimensional non-exchangeable NMR of HP2. Due to poor synthesis yields, only a 0.2 mM sample was obtained for this hairpin, therefore, only one-dimensional spectra were collected. The only conclusive data is that HP2 contains two upfield shifted resonances in the exact places that correspond to the C5H5′/H5″ shifts in HP3, and there appear to be two extra J-coupled resonances in the H1′-H5 region of the spectrum which correlate with the J-coupled H1′ resonances corresponding to the 2 C2′-endo sugars U4 and C5. Based on this evidence, HP2 may have the same loop structure as that found in HP3 and the 12mer.

One and two dimensional NMR of the UACG tetraloop. One-dimensional NOE experiments in water showed the G–U

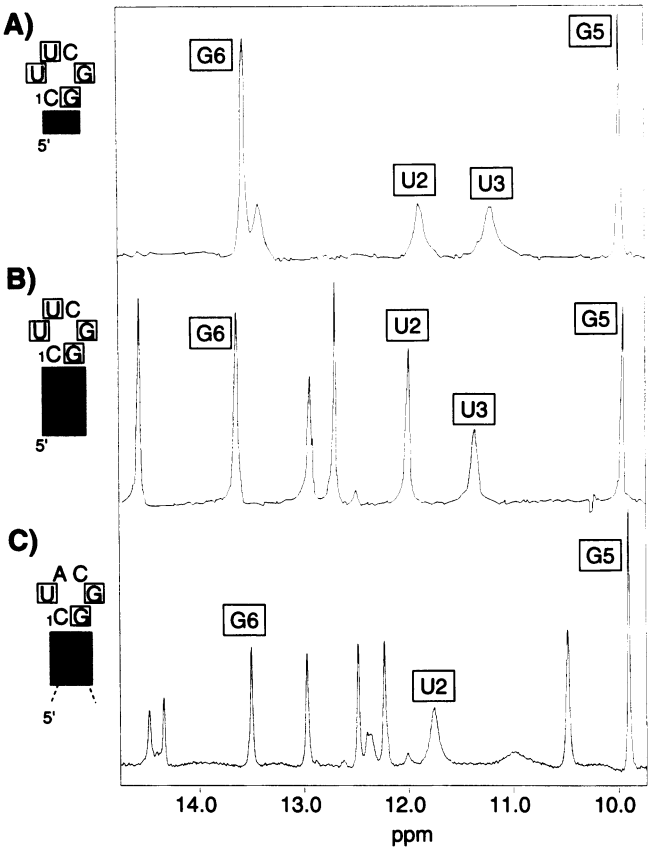

Figure 6. Imino comparison for HP3, UUCG 12mer, and UACG tetraloops. (**A**) HP3 imino spectral with assignments at 15°C, boxed nucleotides refer to comparable nucleotides between spectra. (**B**) UUCG 12mer imino spectrum at 5°C. (**C**) UACG 25mer imino spectrum at 15°C. HP3 and UUCG 12mer are both in 10 mM sodium phosphate, 10 μM EDTA, pH 6.8 and 6.5 respectively. The UACG 25mer has 50 mM sodium chloride also present, pH 6.4.

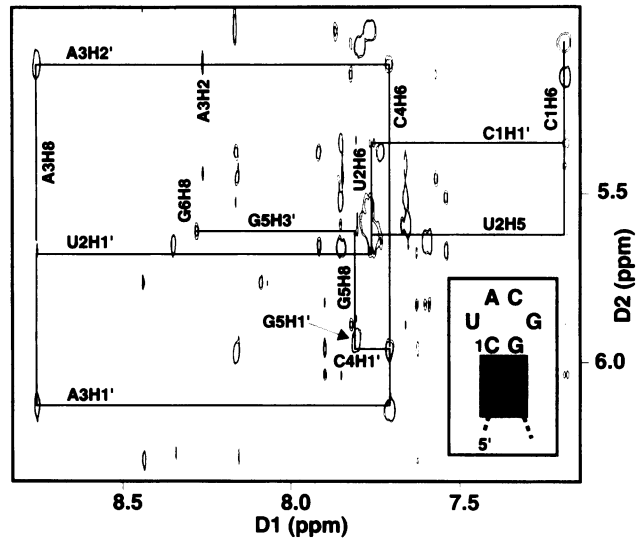

Figure 7. Aromatic to H1′ NOESY region of the UACG 25mer. Lines represent connectivities seen for the loop and closing base pair. Numbering is according to Figure at lower right with the first 5′C as number 1. Sample is in 10 mM sodium phosphate, 50 mM sodium chloride, 10 μM EDTA, pH 6.4.

imino NOE transfer characteristic of the G · U pair in the UUCG 12mer. Furthermore, the G and U iminos of the loop and G imino of the closing base pair appeared at shifts very similar to those found in HP3 and in the 12mer (Fig. 6). The two-dimensional DQF-COSY spectrum showed strong H1′-H2′ couplings for the central nucleotides A and C (the chemical shift for the A varied from that of the U it replaced but the C remained in a very similar location), along with the strongly downfield shifted G H3′ (Fig. 5). The C in the center of the loop had the unusual H5′/H5″ crosspeak near 3.6/2.7 p.p.m. which is a very clear marker for the UNCG loop.

In the H8-H1′ region of the NOESY spectrum, a very intense crosspeak for the G in the loop to its own H1′ indicated its syn conformation as characteristic for these loops. The A appeared in a spectrally clear region at 8.7 p.p.m., 0.3 p.p.m. downfield of the nearest peak with its H2 close by at 8.25 p.p.m. (Fig. 7). Overall, the UACG loop appears to have similar structure to the UUCG loop due to numerous characteristics it shares with the 12mer and HP3.

DISCUSSION

Stability of the mini hairpins

We have demonstrated that two base pairs is the minimum requirement for a stable RNA hairpin with the UUCG tetraloop. Previous work on hairpins with only two closing base pairs has shown that DNA hairpins with the GAAA tetraloop melt at 76.5°C (19), but the RNA equivalent is much less stable with a T_m of 39°C (19). The equivalent stem with the UUCG loop gives a T_m of 55°C, providing clear evidence of the extra stability of the UUCG versus GAAA loops in RNA molecules. Based on previous comparisons of tetraloop stabilities (20) the UNCG loop tends to be more stable in the RNA form than in DNA. As expected, the most stable closing base-pair is a C · G. Somewhat unexpected is the greater ΔG° for HP2 as compared to HP3 which might be explained by greater base stacking on the 3′ end when three purines are found in a row (HP2) compared to two purines and one pyrimidine (HP3). Overall, the stability differences, in terms of ΔG°, are well predicted suggesting that the variability seen is due to stacking differences between nearest neighbors. The stability of these very small hairpins makes them ideal in bringing together RNA strands which may otherwise not pair favorably or which may form multiple structures. Statistical analyses of 16S-like sequences show that UNCG hairpins are most frequently composed of 3, 2 or 7 stem base pairs, in that order (21). Our thermodynamic data is consistent with the two basepair hairpin being very stable. Also, our data further validates secondary structure calculation programs (22) which predict the existence of such small stemmed hairpins within larger structures.

Structural similarity within the UNCG family

Based on the evidence presented, there is little doubt that the UUCG loop in HP3 is very similar structurally to the UUCG loop found in the 12mer. The majority of information which allowed

the determination of the 12mer hairpin structure; strongly shifted resonances, a few crucial NOEs, C2′-endo sugar puckers and NOE intensities, is also present in HP3. The data presented for HP6 and HP2 also suggest the presence of an equivalent loop structure.

The evidence for the UACG loop with a three base pair stem, also appears strongly in favor of a similar structure to the UUCG previously studied. Thermodynamic data on the loop place its T_m above 60°C, as would be expected with three base pairs. The NMR data are overwhelmingly similar for all loop nucleotides other than the A in the loop. Since its position would be out of the loop, as seen for the second U in UUCG (11), it is not surprising that it would perturb the overall structure only slightly.

NMR markers in the UNCG family

The UNCG family of loops provides very simple, clear markers that establish the existence of a hairpin while providing a convenient place to start chemical shift assignments. In exchangeable spectra, its shifts are characteristic and in usually uncrowded areas (Fig. 6). A general method for determining whether the duplex is forming instead of the hairpin involves ^{15}N labeling to unambiguously determine if this is the case (23) . A much simpler method, which is specific for the UUCG hairpin, relies on the observation that the G imino in the loop will shift from 9.9 to 10.8 p.p.m. if in the duplex form (observed by Dr Hal Lewis for the UUCG hairpin and duplex, pers. comm.). The characteristic central two C2′-endo sugars and shifted GH3′ of the loop show themselves very clearly (Fig. 5) with minor variations between the UUCG and UACG tetraloops. The UACG loop has the added benefit of the AH8's downfield shift at 8.7 p.p.m. along with its AH2 at 8.25 p.p.m.; these provide clear markers and reduce crowding in the rest of the aromatic region. The NOE walk seen for the loop is characteristic and easily identified for the UACG 25mer (Fig. 7). Even with variations in pH (6.0–7.3), salt conditions (0–100 mM sodium chloride) and temperature (5–30°C) (Dr M. Chastain, pers. comm.), the UNCG tetraloops show minimal change in chemical shifts resulting in the retention of their clear spectroscopic patterns. On the other hand, GAAA and GCAA loops are not as favorable. Chemical shifts change by >0.1 p.p.m. and peaks vary widely in intensity, with the small changes in salt and pH mentioned above (Dr M. Chastain, pers. comm.). Though the GAAA and GCAA loops are probably not ideal in spectroscopic situation where only one hairpin is needed to secure structure, the GAAA loop has been used along with a UACG tetraloop in our laboratory repeatedly with success (3, unpublished results). Using two UACG loops may prove even better due to exact overlap of loop resonances if the two base pairs immediate to the loop are equal in sequence.

CONCLUSIONS

The UNCG family of ultra stable tetraloop hairpins can have a T_m >50°C with only a two base pair stem. The two base pair hairpins appear to be very similar in structure, as seen by NMR, to the four base pair stem UUCG structure previously solved in our laboratory. The high stability observed for the two base pair stem UUCG hairpins makes them very useful structural elements for producing the desired folding of an RNA. Also, the UUCG and UACG hairpins have very clear spectral markers which identify their conformation as well as providing starting points for chemical shift assignments. The downfield shift of the AH8 and AH2 of the UACG loop make it the best choice for NMR structural studies.

ACKNOWLEDGEMENTS

It is a pleasure to thank Mr David Koh for synthesizing DNA templates and RNA mini hairpins, Dr Gabriele Varani for NMR expertise and initial help on the project, Dr Hal Lewis for chemical shift information for the UUCG duplex, Ms Barbara Dengler for managing the laboratory and Mr K. Y. Chang for helpful encouragement. The research was supported in part by grants from the National Institute of Health (GM 10840), from the Department of Energy (DE-FG03-86ER60406) and instrumentation grants from the Department of Energy and from the National Science Foundation (DOE DE-FG05-86ER75281, NSF DMB 86-09305 and NSF BBS 86-20134).

REFERENCES

1 Szewczak, A. A., Moore P. B., Chang Y. L. and Wool I. G. (1993) *Proc. Natl. Acad. Sci. USA*, **90**, 9581–9585.
2 Wimberly, B., Varani G. and Tinoco I. Jr (1993) *Biochemistry*, **32**, 1078–1087.
3 Chastain, M. and Tinoco I. Jr (1992) *Biochemistry*, **31**, 12 733–12 741.
4 Puglisi, J. D., Wyatt J. R. and Tinoco I. Jr (1990) *J. Mol. Biol.*, **214**, 437–453.
5 Wimberly, B. (1992) Ph.D. Thesis, University of California, Berkeley.
6 Puglisi, J. D., Tan R., Calnan B. J., Frankel A. D. and Williamson J. R. (1992) *Science*, **257**, 76–80.
7 Battiste, J. L., Tan R., Frankel A. D. and Williamson J. R. (1994) *Biochemistry*, **33**, 2741–2747.
8 Peterson, R. D., Bartel D. P., Szostak J. W., Horvath S. J. and Feigon J. (1994) *Biochemistry*, **33**, 5357–5366.
9 Koizumi, M., Kamiya H. and Ohtsuka E. (1993) *Biol. Pharm. Bull.*, **16**, 879–883.
10 Tuerk, C., Gauss P., Thermes C., Groebe D. R., Gayle M., Guild N., Stormo G., d'Aubenton-Carafa Y., Uhlenbeck O. C. and Tinoco I. Jr. (1988) *Proc. Natl. Acad. Sci. USA*, **85**, 1364–1368.
11 Varani, G., Cheong C. and Tinoco I. Jr (1991) *Biochemistry*, **30**, 3280–3289.
12 Hines, J. V., Varani G., Landry S. M. and Tinoco I. (1993) *J. Am. Chem. Soc.*, **115**, 11 002–11 003.
13 Cheong, C., Varani G. and Tinoco I. Jr (1990) *Nature*, **346**, 680–682.
14 Wyatt, J. R., Chastain M. and Puglisi J. D. (1991) *Biotechniques*, **11**, 764–769.
15 Wyatt, J. R. (1990) Ph.D. Thesis, University of California, Berkeley.
16 Shaka, A. J., Barker P. B. and Freeman R. (1985) *J. Mag. Res.*, **64**, 547–552.
17 Puglisi, J. D. and Tinoco I. Jr (1989) *Methods Enzymol.*, **180**, 304–325.
18 Varani, G. and Tinoco I. Jr (1991) *Quart. Rev. Biophys.*, **24**, 479–532.
19 Hirao, I., Nishimura Y., Tagawa Y., Watanabe K. and Miura K. (1992) *Nucleic Acids Res.*, **20**, 3891–3896.
20 Antao, V. P., Lai S. Y. and Tinoco I. Jr (1991) *Nucleic Acids Res.*, **19**, 5901–5905.
21 Wolters, J. (1992) *Nucleic Acids Res.*, **20**, 1843–1850.
22 Zuker, M., Jaeger J. A. and Turner D. H. (1991) *Nucleic Acids Res.*, **19**, 2707–2714.
23 Aboul-ela, F., Nikonowicz E. P. and Pardi A. (1994) *FEBS Lett.*, **347**, 261–264.
24 Turner, D. H. and Sugimoto N. (1988) *Annu. Rev. Biophys. Chem.*, **17**, 167–192.
25 Freier, S. M., Alkema D., Sinclair A., Neilson T. and Turner D. H. (1985) *Biochemistry*, **24**, 4533–4539.
26 Jaeger, J. A., Turner D. H. and Zuker M. (1989) *Proc. Natl. Acad. Sci. USA*, **86**, 7706–7710.